STARS

University of Central Florida
STARS

Faculty Bibliography 1990s | Faculty Bibliography

1-1-1994

Ultrafast Nonlinearities In Semiconductor-Laser Amplifiers

M. Sheik-Bahae

E. W. Van Stryland
University of Central Florida

Find similar works at: https://stars.library.ucf.edu/facultybib1990
University of Central Florida Libraries http://library.ucf.edu

This Article is brought to you for free and open access by the Faculty Bibliography at STARS. It has been accepted for inclusion in Faculty Bibliography 1990s by an authorized administrator of STARS. For more information, please contact STARS@ucf.edu.

Recommended Citation

Sheik-Bahae, M. and Van Stryland, E. W., "Ultrafast Nonlinearities In Semiconductor-Laser Amplifiers" (1994). *Faculty Bibliography 1990s*. 1174.
https://stars.library.ucf.edu/facultybib1990/1174

University of Central Florida
STARS Showcase of Text, Archives, Research & Scholarship

PHYSICAL REVIEW B VOLUME 50, NUMBER 19 15 NOVEMBER 1994-I

Ultrafast nonlinearities in semiconductor laser amplifiers

M. Sheik-Bahae
Department of Physics and Astronomy, University of New Mexico, Albuquerque, New Mexico 87131

E. W. Van Stryland
Center for Research and Education in Optics and Lasers, University of Central Florida, Orlando, Florida 32816
(Received 10 January 1994; revised manuscript received 1 June 1994)

The bound-electronic optical nonlinearities in highly excited semiconductors (i.e., semiconductor lasers) have been calculated using a two-parabolic-band model. The nonlinear absorption spectrum is first obtained using a dressed-state formalism taking into account the contributions from two-photon absorption, electronic Raman, and optical Stark effects. The nonlinear refractive index (n_2) is then found by performing a Kramers-Kronig transformation on the nonlinear absorption spectrum. It is also shown that the quadratic Stark splitting of the bands leads to a shift in the quasi-Fermi levels, which introduces additional absorptive and refractive nonlinearities. The sign, magnitude, and the current-density dependence of the calculated n_2 agree well with some recently published experimental results for Al-Ga-As and In-Ga-As-P diode lasers.

I. INTRODUCTION

Ultrafast, large nonlinear refraction in semiconductor diode lasers at wavelengths near their transparency point has been recently reported.[1–4] Measurements of the dynamics of such nonlinearities have revealed interesting transient effects indicative of various electronic scattering mechanisms.[1–6] The magnitude and ultrafast nature of the observed nonlinear refraction at the transparency point of diode lasers have made them viable candidates for all-optical-switching (AOS) devices.

For bulk semiconductor devices, recent theoretical and experimental studies of nonlinearities in the transparency regime ($\hbar\omega < E_g$) have indicted that at photon energies above half the band gap ($\hbar\omega > E_g/2$) parasitic losses due to two-photon absorption (2PA) hinder the effectiveness of these materials for AOS applications.[7,8] The theory predicts that, as $\hbar\omega \rightarrow E_g$, n_2 is resonantly enhanced but 2PA remains relatively constant leading to favorable conditions for low-power AOS.[8] In practice, however, the presence of linear loss due to band-tail absorption and the consequent band-filling effects rule out near-resonant AOS operation in passive materials. Recent experiments[1–4] suggest that a possible solution to this problem is to suppress the linear absorption by injecting a nonequilibrium electron-hole population and operating in the spectral region where the net absorption is negligible, i.e., the transparency point. In this paper, we will examine ultrafast bound-electronic nonlinearities in semiconductors in the presence of a nonequilibrium plasma using a simple two-band model. The injection of a high electron-hole density, however, is accompanied by additional dynamics arising from large intraband (free-carrier absorption) as well as interband transitions. The dynamics of such real excitations have been recently studied in detail elsewhere.[5] With ultrashort pulses ($\simeq < 100$ fs), additional dynamics due to spectral hole burning have been observed.[6] Effects of spectral hole burning are still present around the transparency point, even though no or little net exchange of electron-hole population between the conduction and valence bands occurs. In a time-resolved experiment, one may distinguish the real excitation processes from the ultrafast virtual excitations by recognizing the much longer energy relaxation times associated with the real excitation. The characteristic energy relaxation times are $\simeq 1-2$ ps for intraband and $\simeq 100$ ps-100 ns for interband transitions.[9] It should be noted, however, that spectral hole burning has a lifetime of the order of 100 fs and may behave similarly to the bound-electronic nonlinearity, making experimental interpretation more complicated.[6]

The purpose of this paper is to analyze bound-electronic contributions to the nonlinear processes while ignoring real excitation effects. This work complements studies of the real excitation (carrier) nonlinearities.[6] We study virtual processes using a simple two-parabolic-band (TPB) model for semiconductors under nonequilibrium population conditions while assuming a cw (adiabatic) perturbation by the optical fields. The formalism used here is an extension of our earlier model,[8] which successfully described the dispersion and band-gap scaling of the electronic n_2 in passive semiconductors in their transparency range.

We use a nonlinear Kramers-Kronig transformation[8,10] to obtain the nonlinear refractive index n_2 from the calculated first-order nonlinear absorption coefficient α_2:

$$n_w(\omega) = \frac{c}{\pi}\int_0^\infty \frac{\alpha_2(\omega';\omega)}{\omega'^2-\omega^2}d\omega' , \tag{1}$$

where α_2 is defined as $\Delta\alpha/I$ with $\Delta\alpha(\omega;\omega')$ representing any change in the absorption coefficient at ω' induced by the presence of an excitation at ω with irradiance I. Our task is to calculate this change in the absorption spectrum caused by virtual excitation at ω. In Ref. 8 we showed that by using a Volkov-type dressed Bloch func-

0163-1829/94/50(19)/14171(8)/$06.00 ©1994 The American Physical Society

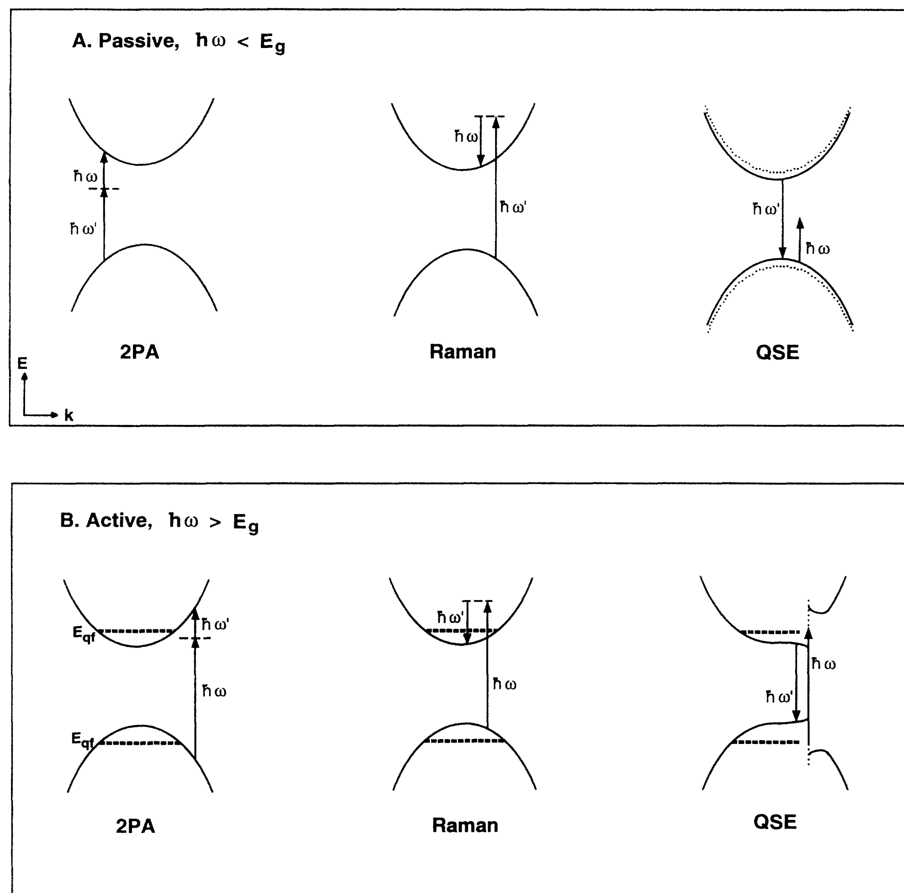

FIG. 1. Diagrammatical representation of the nonlinear absorption due to two-beam interaction in a two-band system for (a) passive semiconductor and excitation photon energy $\hbar\omega < E_g$, and (b) active semiconductor with $\hbar\omega > E_g$.

tion we can account for all the possible mechanisms (in a TPB model) that lead to a change of absorption that varies linearly with the excitation irradiance. These mechanisms include 2PA (when $\hbar\omega' > E_g - \hbar\omega$), electronic Raman (when $\hbar\omega' > E_g + \hbar\omega$), and optical Stark effect (for $\hbar\omega' > E_g$). A diagrammatic representation of these processes is depicted in Fig. 1(a) for a passive material with excitation in the transparency region ($\hbar\omega < E_g$). A similar physical description can be given for a system having a quasiequilibrium electron-hole population (i.e., with gain), and above-resonance excitation ($\hbar\omega > E_g$). This is illustrated in Fig. 1(b) for a simple two-band system. In this case there are spectral regions where the probe will experience a two-photon and/or Raman gain rather than absorption. The quadratic optical Stark effect (QSE) as qualitatively depicted in Fig. 1(b) exhibits a particularly interesting behavior. The existence of above-band-gap excitation results in the formation of additional energy gaps (light-induced gaps[11]) in both the valence and conduction bands. We will show later that this effect may redshift the transparency point once the quasiequilibrium is reestablished. A dynamic shift of the transparency point, and, in general, any above-band-gap excitation, can lead to additional real excitation processes that, as discussed earlier, are distinguished from ultrafast virtual processes by their longer recovery times.[1] In modeling described in the following section, we separate the virtual processes by considering only coupling between those states whose virtual carrier lifetime (inverse detuning) is shorter than the phenomenological dephasing time (T_2). It must be emphasized that this simple model aims at explaining the observed bound-electronic nonlinearities at or near transparency where the effects of real excitation (or deexcitation) are negligible. A detailed understanding of the dynamics of the optical nonlinearities, particularly at spectral regions where the optical field experiences strong absorption or gain, requires more rigorous time-evolution analysis containing Bloch equations.

II. NONLINEAR ABSORPTION SPECTRUM

A detailed description of the TPB theory of nonlinear absorption and n_2 in the transparency region has been given in Refs. 8 and 12. A succinct review of this theory follows. The optical interaction is via the $(e/c)\mathbf{A}\cdot\mathbf{p}$ Hamiltonian where $\mathbf{a} = \mathbf{A}_0' \cos(\omega'\tau) + \mathbf{A}_0 \cos(\omega\tau)$ represents the total vector potential and $\mathbf{p} = i\hbar\nabla$ denotes the momentum operator. The nonlinear interaction is formulated in two steps. In the first step the optical fields alter the energy of the electrons in both initial and final states by virtue of the linear and quadratic Stark effects. In the second step, the transition rate between these "dressed" states (bands) is calculated using first-order

perturbation theory. The linear and quadratic Stark effects are incorporated into the band states via their energies given by

$$E_{c,v}=E^0_{c,v}-\frac{e\hbar}{m_{c,v}c}\mathbf{k}\cdot\mathbf{A}(\tau)\pm\Delta E^{\mathrm{QSE}}_{cv}\ , \qquad (2)$$

where $\mathbf{k}$ is the electronic wave vector, $E^0_{c,v}$ is the unperturbed energy of the valence (v) or conduction (c) band, and $m_{c,v}$ denotes the effective mass of the corresponding band. The first correction term in energy is time dependent and corresponds to the linear optical Stark effect (LSE). This is a time-varying (oscillating) energy term and leads to absorptive changes that involve the loss or emission of the excitation photons, i.e., 2PA and Raman effects.[8,12] The second term is the QSE energy shift that is positive for the conduction band and negative for the valence band. We assume, for simplicity, two parabolic bands with equal curvature; thus $m_c=m_v=m_0E_g/E_p$, where m_0 is the free-electron mass and E_p is the Kane energy which is nearly constant ($\simeq 20$ eV) for most semiconductors.[13]

It is important to keep in mind that the field at ω is assumed to be the strong excitation field while the probe at ω' is regarded as weak. Hence we consider $\Delta E^{\mathrm{QSE}}_{c,v}$ due to excitation by the field $\mathbf{A}_0$ only:[8]

$$\Delta E^{\mathrm{QSE}}_{cv}(\mathbf{k})=\left|\frac{e\,\mathbf{A}_0\cdot\mathbf{p}_{cv}}{2m_0c}\right|^2\mathrm{Re}\left\{\frac{1}{E_{cv}-\hbar\omega+i2\hbar\Gamma}+\frac{1}{E_{cv}+\hbar\omega+i2\hbar\Gamma}\right\}, \qquad (3)$$

where $E_{cv}(\mathbf{k})$ is the valence- to conduction-band energy difference with parabolic dispersion and $\mathbf{p}_{cv}$ is the interband momentum matrix element. Because of on-resonance excitation imposed by the condition $\hbar\omega>E_g$, we have included a broadening term associated with scattering frequency $\Gamma=1/T_2$, where T_2 is the phenomenological dephasing time of the electrons (or holes). By this definition, the combined electron-hole scattering rate, associated with the interband transition, is 2Γ. The inclusion of T_2 implies that only excitations into $\mathbf{k}$ states with an inverse detuning ($|\omega-E_{cv}/\hbar|^{-1}$) shorter than T_2 are accounted for, and real excitations that lead to long-lived carrier effects are excluded. We assume a constant-T_2 approximation and ignore the energy or detuning dependence of this quantity.[14] The influence of broadening on the first-order energy shift in Eq. (2) can be approximated using the classical transformation of the vector potential from $\mathbf{A}(t)$ into $\mathbf{A}(t)-\Gamma\int_0^\infty \mathbf{A}(t+\tau)e^{-\Gamma\tau}d\tau$ under a momentum relaxation rate of Γ. Strictly speaking, formulating the scattering effects in the above manner implies a steady-state situation. Thus we cannot accurately analyze but only speculate about the transient effects occurring within the time T_2.

The second step in the interaction is to calculate the transition rate between the two dressed states using first-order perturbation theory. Separating out the components that vary linearly with the excitation irradiance and involve the absorption or emission of a single photon of the probe ($\hbar\omega'$), we obtain the nondegenerate absorption coefficient

$$\alpha_2(\omega';\omega)=K\frac{\sqrt{E_p}}{n_{01}n_{02}E_g^3}\tilde{F}_2(\hbar\omega'/E_g;\hbar\omega/E_g)\ , \qquad (4)$$

where $K=2^9\pi e^4/5c^2\sqrt{m_0}$ and n_{0j} ($j=1,2$) are the linear refractive indices at the probe and excitation wavelengths, respectively.[8] The function $\tilde{F}_2$ contains information about the optically coupled states as well as the gain/loss characteristic of the system and is given by

TABLE I. The nonlinear absorption spectrum function F_2. The terms $(\cdots)^{3/2}$ and $(\cdots)^{\mp 1/2}$ are zero when their argument is negative. The sign of the Raman term is determined by the sign of (x_1-x_2). Here $\gamma=\hbar/E_gT_2$.

Contribution	$F_2^i(x_1;x_2)$
2PA	$\frac{(x_1+x_2-1)^{3/2}}{2^7x_1x_2^2}\frac{(x_1+x_2)^2}{(x_1^2+\gamma^2/4)(x_2^2+\gamma^2/4)}$ for $x_1+x_2>1$
Raman	$\pm\frac{(\lvert x_1-x_2\rvert-1)^{3/2}}{2^7x_1x_2^2}\frac{(x_1-x_2)^2}{(x_1^2+\gamma^2/4)(x_2^2+\gamma^2/4)}$ for $\lvert x_1-x_2\rvert>1$
Linear Stark	$-\frac{(x_1-1)^{3/2}}{2^6x_1x_2^2}\frac{x_1^2}{(x_1^2+\gamma^2/4)(x_2^2+\gamma^2/4)}$ for $x_1>1$
Quadratic Stark	$-\frac{1}{2^{10}x_1x_2^2(x_1-1)^{1/2}}\left[\frac{x_1-x_2}{(x_1-x_2)^2+\gamma^2}+\frac{x_1+x_2}{(x_1+x_2)^2+\gamma^2}-\frac{2(x_1-1)[(x_1-x_2)^2-\gamma^2]}{[(x_1-x_2)^2+\gamma^2]^2}-\frac{2(x_1-1)[(x_1+x_2)^2-\gamma^2]}{[(x_1+x_2)^2+\gamma^2]^2}\right]$ for $x_1>1$

$$\tilde{F}_2 = F_2^{\zeta}(x_1;x_2)\{f_c - f_v\} \; , \quad (5)$$

where $\{f_v - f_c\}$ is the occupancy factor with $f_{c,v}$ denoting the quasiequilbrium Fermi-Dirac distribution functions for conduction and valence bands, respectively. The spectral function F_2^{ζ} contains the contributions from 2PA, electronic Raman, and optical Stark effects. This function, which is essentially an energy-broadened version of the function F_2 derived in Ref. 12, is given in Table I. Assuming equal quasi-Fermi levels for the electrons and holes, we write the occupancy factor as

$$\{f_c - f_v\} = \frac{\sinh(\nu_m)}{1+\cosh(\nu_m)} \; , \quad (6)$$

where

$$\nu_m = \frac{|m\hbar\omega + \hbar\omega'| - 2E_{\rm QF}}{2k_B T}$$

with $m = 1, -1, 0$ corresponding to 2PA, Raman, and optical Stark effects, respectively. T is the carrier temperature and k_B is the Boltzman constant. The quasi-Fermi level $E_{\rm QF}$ is referenced to the midgap ($E_g/2$) energy, i.e., $E_{\rm QF} \simeq 0$ for an intrinsic, passive material. We define the transparency point to occur at $\hbar\omega_{\rm tr} = 2E_{\rm QF}$ for a system with gain ($E_{\rm QF} > 0.5E_g$). After normalizing all the energy parameters with respect to E_g, we can rewrite ν_m as

$$\nu_m = (|x_1 + m x_2| - x_{\rm tr})/2\eta \; , \quad (7)$$

where $\eta = k_B T/E_g$ and $x_{\rm tr} = \hbar\omega_{\rm tr}/E_g$. Figure 2(a) (solid lines) shows the absorption $\alpha_2(\omega';\omega)$ calculated separately for each mechanism assuming $E_{\rm QF} = 0.515E_g$ (i.e., $x_{\rm tr} = 1.03$). Figure 2(b) (solid line) depicts the total change of absorption in the vicinity of the transparency point. The effects of Raman and 2PA are manifested as a net increase in the absorption. This absorption increases as the probe frequency is reduced [Fig. 2(a)]. On the other hand, the QSE contribution is more localized in energy since the optical field induces a gap that alters the density of states only in the vicinity of the excitation photon energy $\hbar\omega$. An important consequence of this induced change in the density of states is the self-adjustment of the quasi-Fermi levels (on a time scale of carrier-carrier scattering times) in order to conserve the total carrier density. This leads to an additional contribution to α_2 and hence alters the total absorption spectrum as shown by the dashed lines in Figs. 2(a) and 2(b). In the following section we give a simple derivation of this quasi-Fermi energy shift and the resultant change of absorption.

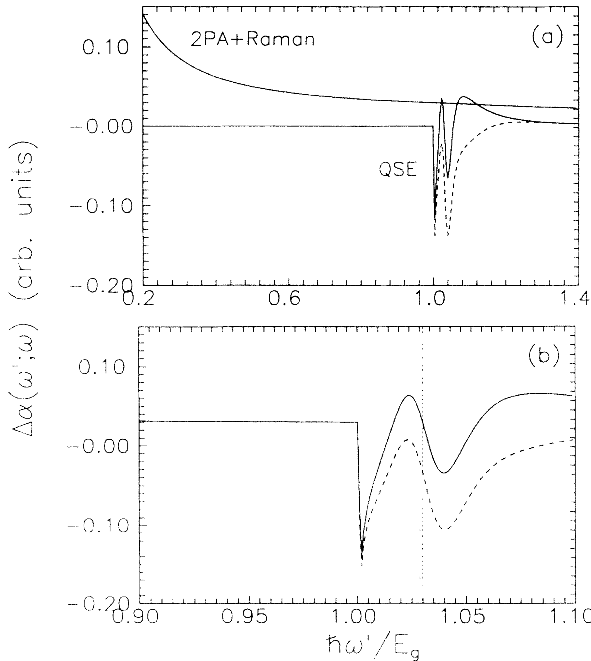

FIG. 2. (a) The calculated change in absorption due to virtual excitation at the transparency wavelength ($\hbar\omega/E_g = 1.03$) due to various mechanisms. (b) The total absorption as the sum of these contributions plotted in the vicinity of the transparency point (vertical dashed line). The solid and dashed lines correspond to unshifted and shifted quasi-Fermi levels, respectively.

III. STARK SHIFT OF THE QUASI-FERMI LEVELS

A consequence of the modulation of the band curvature due to the QSE, as given by Eq. (2), is the change of the local density of states. For example, as was shown diagrammatically in Fig. 1, this effect reduces the density of states in the center of the induced gap but increases it above and below center. To illustrate this effect, we calculate the density of states

$$N_{c,v}(E) = 1/4\pi^3 \int d\mathbf{k}\, \delta[E - E_{c,v}]$$

for each band using the band energy dispersions given by Eqs. (2) and (3). Figure 3 shows the calculated $N_c(E)$ in the presence of the QSE as compared to the well-known square-root dependence ($\sqrt{E - E_g}$) of a nonperturbed band. The perturbing field used to calculate $N_c(E)$ in Fig. 3 was chosen to be large enough to overemphasize the induced change. As we shall see, this modulation in the

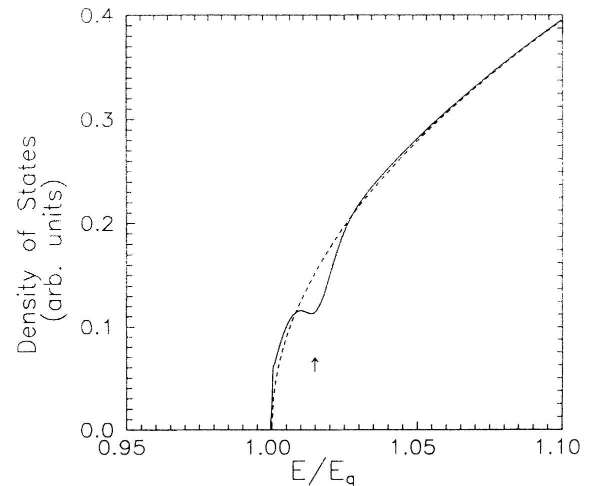

FIG. 3. The density of states versus energy for a parabolic band under quadratic Stark effect (solid line). The dashed line is the square-root function of a nonperturbed band. The arrow indicates the photon energy of the excitation.

density of states significantly alters the quasi-Fermi levels only when the excitation is very near the transparency point which is precisely the situation we are most concerned with in this paper. The shift in E_{QF} can be viewed as a process to ensure the conservation of the total carrier density in the absence of a net population exchange. This adjustment is not instantaneous and has a characteristic time determined by the carrier-carrier scattering time ($\tau_{e-e} \simeq 100$ fs),[15] after which the Fermi distribution is reestablished. The energy shift (ΔE_{QF}) can be obtained from the Fermi integral for the total electron (or hole) density:

$$\int f(E_c(\mathbf{k}) - E_{QF} - \Delta E_{QF}) d\mathbf{k} = \text{const} , \tag{8}$$

where E_c is given by Eq. (2) and $f(\epsilon) = (1 + e^{-\epsilon/k_B T})^{-1}$ is the Fermi distribution function. Using a variational procedure, we solve Eq. (8) for ΔE_{QF} to first order in the excitation irradiance I and obtain

$$\Delta E_{QF} = BI \frac{E_p}{n_0 E_g^3} T(\hbar\omega / E_g) , \tag{9}$$

where $B = 2^{10}\pi e^2 \hbar^2 / 5 m_0 c$ and $T(x_2)$, which contains the spectral dependence of this energy shift, is given by

$$T(x_2) = \frac{\int_1^{\infty} F_2^{QSE}(x_1; x_2) f((x_1 - x_{tr}) E_g / 2) x_1 dx_1}{\int_1^{\infty} (x_1 - 1)^{1/2} [\partial f((x_1 - x_{tr}) E_g / 2) / \partial x_1] dx_1} . \tag{10}$$

Here F_2^{QSE} corresponds to the broadened QSE spectral function given in Table I. It is worth noting that, just as the absorption change due to the QSE is the virtual analog of spectral hole burning (band blocking), the consequent shift of the quasi-Fermi levels is effectively a virtual analog to a similar effect arising from carrier heating that follows the hole-burning process. Thus one may regard the shift of the quasi-Fermi levels as given by Eq. (10) as a "virtual carrier heating" effect.

Figure 4 shows $T(x_2)$ calculated as a function of the excitation photon energy $\hbar\omega/E_g$ assuming quasi-Fermi levels corresponding to $\hbar\omega_{tr}/E_g = 1.03$ and 1.05. Note that the general features of $T(x_2)$ do not strongly depend on the initial E_{QF} although the shift at the transparency point is smaller with a larger initial E_{QF}. It is evident from Fig. 4 that E_{QF}, and hence the transparency point, is blueshifted for below and around transparency excitation, but as $\hbar\omega$ exceeds $\hbar\omega_{tr}$, the sign of ΔE_{QF} ultimately reverses, resulting in a redshift of the transparency point. Of practical importance is the situation when excitation is at the transparency point. According to Fig. 4, there is a blueshift of E_{QF} which results in a net decrease of the absorption coefficient, since $\hbar\omega$ now overlaps the gain region. The effective α_2 coefficient associated with this energy shift is found to be

$$\alpha_2^{QF}(\omega'; \omega) \simeq \frac{\partial \alpha_0(\omega')}{\partial E_{QF}} \frac{\Delta E_{QF}(\omega)}{I} , \tag{11}$$

where α_0 is the linear interband absorption given by

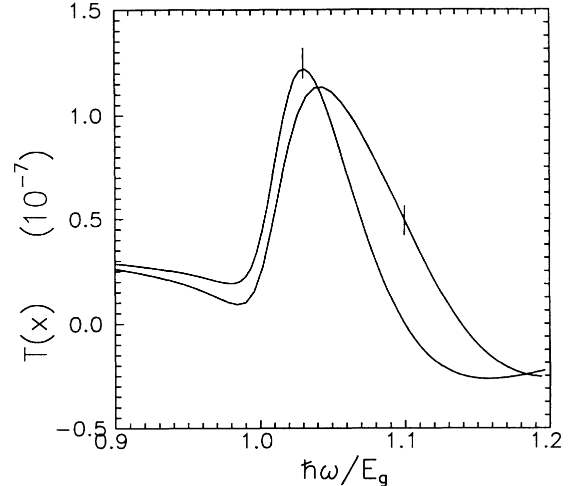

FIG. 4. The calculated shift of the quasi-Fermi levels due to quadratic Stark splitting of the energy bands as a function of excitation photon energy for two values of initial quasi-Fermi levels. The transparency points of each curve at $\hbar\omega_{tr}/E_g = 1.03$ and 1.05 are marked.

$$\alpha_0(\omega') = \frac{e^2 \sqrt{m_0}}{3 c \hbar^2} \frac{E_g}{n_0 \sqrt{E_p}} \frac{(x_1 - 1)^{1/2}}{x_1} \{ f_c - f_v \} . \tag{12}$$

The total change in the absorption spectrum due to the QSE is depicted in Fig. 2(a) (dashed line) as the sum of α_2^{QF} and α_2^{QSE} from Eq. (4). The overall α_2 (assuming quasiequilibrium has been reestablished) is shown in Fig. 2(b) (dashed line) and can be represented by the same relation as in Eq. (4) provided that we modify the $\tilde{F}_2^{QSE}$ in Table I to become

$$\tilde{F}_2^{QSE}|_{total} = \tilde{F}_2^{QSE} - \frac{4T(x_2)}{3\eta} \frac{(x_1 - 1)^{1/2}}{x_1} \frac{1}{1 + \cosh(\nu_0)} .$$

Although the nonlinear response dynamics of such a system requires a more rigorous time-domain analysis (i.e., Bloch equations), we will attempt to infer a qualitative picture for the nonlinear absorption dynamics from the approach presented here. We may conclude from Fig. 2(b) that a probe beam having the same wavelength as the pump will undergo an initial decrease in the transmission due to two-photon absorption. For laser pulses containing many optical cycles, this will appear instantaneous. This will be followed after a time $\tau \simeq \tau_{e-e}$ by an increase of transmission due to the QSE and subsequent blueshift of the quasi-Fermi levels. Although this qualitative description is consistent with certain experimentally observed ultrafast gain dynamics,[2] one cannot generally ignore the real excitation effects such as carrier heating and spectra hole burning in analyzing the experimental data. For example, carrier heating arising from free-carrier absorption (with a rise time comparable to that of the quasi-Fermi-level shift) would tend to redshift the transparency point, thus opposing the effects of the QSE.[2–5]

IV. NONLINEAR REFRACTION

Following Eq. (1), the induced change in the refractive index is now obtained using the Kramers-Kronig (KK) transformation of the calculated nondegenerate $\Delta\alpha$ spectrum. Similar to the case of passive materials,[8] we derive the following formula for the nonlinear index n_2:

$$n_2 \times 10^{-11}(\mathrm{cm^2/W}) = K' \frac{\sqrt{E_p\ (\mathrm{eV})}}{E_g^4\ (\mathrm{eV}) \times n_0^2} G_2(\hbar\omega/E_g)\ , \tag{13}$$

where $K'=\hbar cK/2$ and G_2 is the dispersion function of n_2 related to $\tilde{F}_2$ via the KK integral. Specifically,

$$G_2(x) = \frac{2}{\pi}\int_0^\infty \frac{\tilde{F}_2(x_1;x)}{x_1^2 - x^2} dx_1\ . \tag{14}$$

It is important to note that just as $\tilde{F}_2$ is a function of temperature ($k_B T/E_g$) and broadening ($\hbar/T_2 E_g$), as well as optical frequencies, G_2 will also contain such dependences. This is in contrast to the case of passive materials (at $\hbar\omega < E_g$) where F_2 and G_2 were only functions of frequencies.[8]

Since the KK integral represents essentially a linear transformation, the G_2 function corresponding to each of the mechanisms involved in the absorptive process can be separately evaluated by using the relevant $\tilde{F}_2$ function in Eq. (14). Figure 5 depicts the calculated G_2 functions corresponding to the different absorptive contributions in Fig. 2 at a transparency point of $x_{tr}=1.03$. Note that the magnitude of G_2 due to the QSE is small initially (solid line) before allowing for the shift in the quasi-Fermi levels. This means that n_2 is initially dominated by two-photon effects (2PA + Raman). Figure 6 shows the total G_2 function for various quasi-Fermi levels corresponding to different injection current levels in a diode laser, with the transparency points indicated. The dispersion curves in Fig. 6 contain the total contributions from 2PA, Raman, and the QSE (including the quasi-Fermi-level shift), and all have a negative sign at the transparency point.

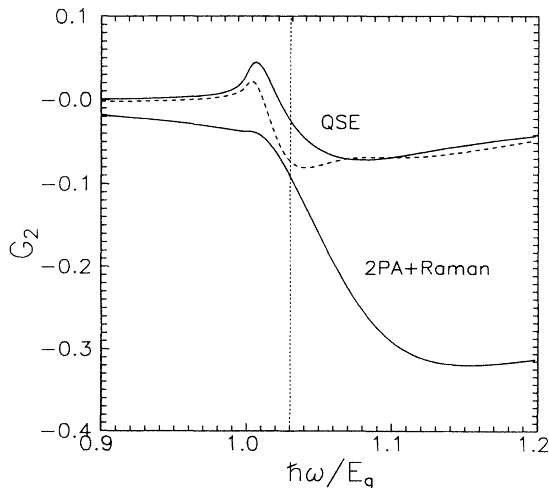

FIG. 5. The calculated dispersion function of n_2 due to various mechanisms. The contribution from QSE is shown for unshifted (solid line) and shifted (dashed line) quasi-Fermi levels.

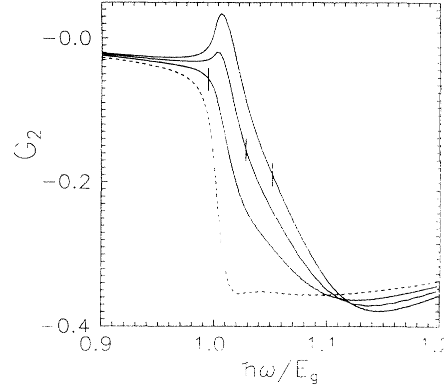

FIG. 6. The calculated total G_2 dispersion function for various quasi-Fermi levels. The dashed line represents G_2 for a passive semiconductor. The transparency point of each curve (at $\hbar\omega/E_g=1.0$, 1.03, and 1.05) is marked.

For the remainder of the paper, we will refer to G_2 as the total contribution, accounting for the shift in the quasi-Fermi levels.

Also evident from Fig. 6 is the moderate increase in magnitude of n_2 at the transparency point as the E_{QF} is raised, i.e., injection current is increased. This dependence is explicitly illustrated in Fig. 7 where the variation

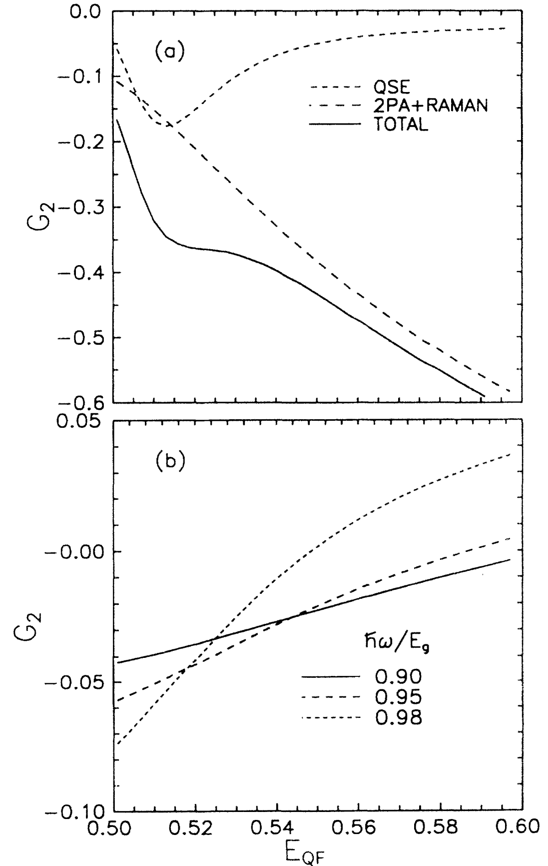

FIG. 7. The variation of G_2 as a function of quasi-Fermi level, E_{QF}, (a) at transparency point ($\hbar\omega=\hbar\omega_t$) with contributions from QSE and 2PA + Raman shown explicitly, and (b) below band edge with $\hbar\omega/E_g=0.9$, 0.95, and 0.98.

of G_2 versus E_{QF} is plotted for photon energies corresponding to the transparency point [Fig. 7(a)] as well as to the below-band-edge region with $\hbar\omega/E_g=0.9$, 0.95, and 0.98. In Fig. 7(a) the separate contributions from QSE and 2PA + Raman are explicitly shown. The vanishing contribution of the QSE as the transparency point moves up in the conduction band is a consequence of equal but opposite-sign contributions due to blueshifting of the states with $E_{cv}>\hbar\omega$ and redshifting of those with $E_{cv}<\hbar\omega$. The main features of Figs. 7(a) and 7(b), namely, the increase in magnitude of n_2 at the transparency point, as well as the reduction of n_2 below the band edge as a function of E_{QF}, are in good agreement with the recently reported experiments.[16]

In calculating the dispersion curves of Fig. 2, we assumed $\eta=0.02$ [defined in Eq. (7)] for the carrier temperature and $\gamma=0.02$ [defined after Eq. (5)] for the broadening. This corresponds to $T_2\simeq130$ fs and $T\simeq350$ K for a semiconductor with $E_g\simeq1.5$ eV (e.g., GaAs). The value of $|G_2|$ at the transparency point increases as these two parameters are reduced, i.e., n_2 is enhanced as the ambient temperature is lowered and/or T_2 is increased. The temperature dependence of G_2 at transparency, calculated for different values of broadening (γ) is shown in Fig. 8. The nature and magnitude of T_2 in semiconductors has been subject to much debate and study in the past. The dephasing time arising from carrier-carrier scattering was recently calculated by Binder *et al.* for highly excited (degenerate) semiconductors.[15] Their results indicated a minimum in the electron-electron scattering rate for k states near the quasi-Fermi wave number, leading to a large T_2 at the transparency point. A qualitative experimental verification of this theory was reported recently.[17] The experiments also showed, in accordance with theory, a much reduced scattering rate at lower temperatures.[15,17] For example, the calculated T_2 for electrons in GaAs at a high plasma density varies from $\simeq100$ fs to $\simeq1$ ps as the temperature is reduced from $T=300$ to 10 K.[15,17] In view of such a temperature dependence, Fig. 8 suggests that a substantial enhancement of n_2 may be observed in laser diodes at low temperatures.

For passive bulk semiconductors, the constant K' was evaluated in Refs. 8 and 12 to be $\simeq6$ [units of Eq. (13)]. However, this underestimated by a factor of $\simeq4$ the n_2 for $Al_xGa_{1-x}As$ samples at wavelengths very near the band edge.[18] In Ref. 12, we suggested that this discrepancy may be partially attributed to the electron-hole Coulomb interaction which has been neglected in the theory. Similarly to the procedure outlined in Ref. 12, we can account for this interaction in the nonlinear absorption spectrum by using an Elliott-type enhancement factor for the continuum of excitons. However, the high plasma densities present in the active semiconductors require that the Coulomb screening of the excitons must also be taken into account. In the following, a correction to α_2 and n_2, due to Coulomb interaction, will be estimated using a simple formalism. We use the screened enhancement factor calculated by Banyai and Koch[19] for the continuum of excitons. We then generalize this procedure and, as given in Ref. 12, apply it to the nonlinear absorption spectrum by multiplying the F_2 functions of each process by the excitonic function $U(\rho_m)$:[19]

$$U(\rho_m)=\prod_{n=1}^{\infty}\left[1+\frac{2gn^2-g^2}{(n^2-g)^2+n^2g^2\rho_m}\right], \tag{15}$$

where g is a screening parameter related to the quasi-Fermi levels as given in Ref. 19 and

$$\rho_m=\frac{|x_1+mx_2|-1}{E_{ex}/E_g}, \tag{16}$$

where E_{ex} is the binding energy of the exciton. Applying this enhancement factor to all the processes involved in the transition rate, we can reevaluate α_2 and n_2. The exciton-enhanced G_2 function obtained using this approximation is shown in Fig. 9 for a typical exciton binding energy of $E_{ex}=0.01E_g$. Although no appreciable qualitative difference is seen, it is evident that more than a two times enhancement of the transparency value of G_2

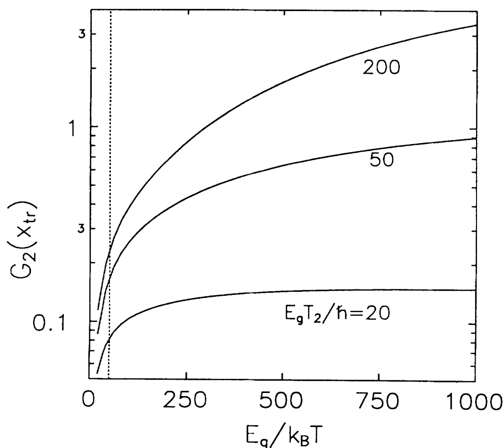

FIG. 8. The temperature dependence of the transparency value of G_2 for various broadening parameters. The vertical dashed line corresponds to $\eta=0.02$ ($k_BT/E_g=50$).

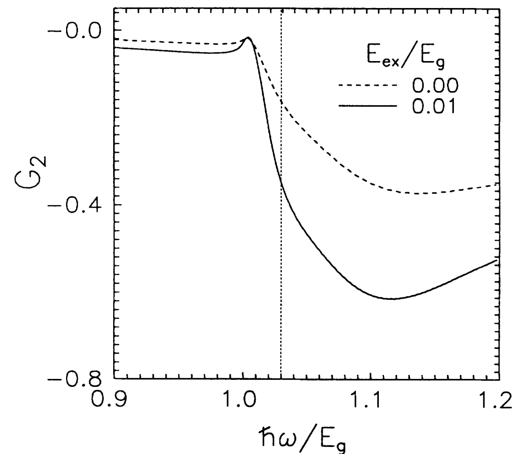

FIG. 9. The calculated n_2 dispersion function including screened exciton enhancement (solid line) in comparison with the no-exciton case (dashed line). The transparency point is at $\hbar\omega/E_g=1.03$.

is predicted. Using the exciton-enhanced G_2 function, we find that the expression in Eq. (13) gives relatively good agreement with the sign and magnitude of the measured n_2 values in $Al_xGa_{1-x}As$ and In-Ga-As-P diode lasers. Using $E_g = 1.5$ and $n_0 = 3.4$ for $Al_xGa_{1-x}As$, we obtain $n_2 \simeq -2\times10^{-12}$ cm^2/W which is in reasonable agreement with the measured value of -5×10^{-12} cm^2/W reported in Ref. 1. The experimentally reported values of n_2 in In-Ga-As-P vary from $|n_2| \simeq (2-4)\times10^{-11}$ using spectral analysis[4] to $n_2 \simeq -3\times10^{-12}$ cm^2/W using a time-division interferometric technique.[2] This large difference may be attributed to difficulties in obtaining accurate effective mode areas for the laser waveguides, as has been pointed out in Ref. 2. Taking $E_g \simeq 0.83$ eV for In-Ga-As-P, we use the E_g^{-4} scaling law in Eq. (13) to obtain $n_2 \simeq -2\times10^{-11}$ cm^2/W, assuming the same G_2 value as in $Al_xGa_{1-x}As$. But considering the dependence of G_2 on T/E_g and $1/T_2E_g$, as given by Fig. 8, we expect the band-gap scaling to be weaker than E_g^{-4} if we assume that the temperature T and dephasing time T_2 are unchanged. From Fig. 8 we see that by lowering E_g by a factor of 2, but keeping T and T_2 constant, a nearly fourfold decrease in the value of G_2 at transparency is estimated. This assumption leads us to estimate $n_2 \simeq -5\times10^{-12}$ for In-Ga-As-P at room temperature. This is well within the range of experimentally reported values.[2,4]

In conclusion, we have obtained a simple expression that gives the dispersion and band-gap scaling of the ultrafast n_2 in semiconductor lasers near their transparency point. We have accounted for the effects of two-photon absorption, electronic Raman, and optical Stark shift, including a self-adjustment of the quasi-Fermi levels.

ACKNOWLEDGMENTS

We gratefully acknowledge the support of the National Science Foundation Grant No. ECS-9120590. The authors also thank Professor Erich P. Ippen and Professor Alan Miller for helpful and enlightening discussions.

[1] C. T. Hultgren and E. P. Ippen, Appl. Phys. Lett **59**, 635 (1991).

[2] K. L. Hall, J. Mark, E. P. Ippen, and G. Eisenstein, Opt. Lett. **576**, 1740 (1990); K. L. Hall, A. M. Darwish, E. P. Ippen, U. Koren, and G. Raybon, Appl. Phys. Lett. **62**, 1320 (1993).

[3] C. T. Hultgren, D. J. Dougherty, and E. P. Ippen, Appl. Phys. Lett. **61**, 2767 (1992).

[4] M. A. Fisher, H. Wickes, G. T. Kennedy, R. S. Grant, and W. Sibbett, Electron. Lett. **29**, 1185 (1993).

[5] P. J. Delfyett, A. Dienes, J. P. Heritage, M. Y. Hong, and Y. H. Chang, Appl. Phys. B **58**, 183 (1994).

[6] B. Flugel, S. W. Koch, and N. Peyghambarian, *Proceedings of the 9th Interdisciplinary Laser Science Conference, Toronto, Canada, 1993* (American Institute of Physics, New York, 1993). See also A. D'Ottavi, E. Iannone, A. Mecozzi, S. Scotti, P. Spano, J. Landreau, A. Ougazzaden, and J. C. Bouley, *Technical Digest of IQEC-94* (Optical Society of America, Washington, D.C., 1994).

[7] V. Mizrahai, K. W. DeLong, G. I. Stegeman, M. A. Saifi, and M. J. Andrejco, Opt. Lett. **14**, 1140 (1989).

[8] M. Sheik-Bahae, D. C. Hutchings, D. J. Hagan, and E. W. Van Stryland, IEEE J. Quantum Electron. **QE-27**, 1296 (1991).

[9] R. Luzzi and A. R. Vasconcellos, in *Semiconductors Probed by Ultrafast Laser Spectroscopy,* edited by R. R. Alfano (Academic, San Diego, 1984), Vol. I.

[10] D. C. Hutchings, M. Sheik-Bahae, D. J. Hagan, and E. W. Van Stryland, Opt. Quantum Electron. **24**, 1 (1992).

[11] H. Haug, *Optical Nonlinearities and Instabilities in Semiconductors* (Academic, San Diego, 1988).

[12] M. Sheik-Bahae, J. Wang, and E. W. Van Stryland, IEEE J. Quantum Electron. **QE-30**, 249 (1994).

[13] E. O. Kane, J.Chem. Phys. Solids **1**, 249 (1957).

[14] M. G. Burt, Semicond. Sci. Technol. **5**, 1215 (1990); **8**, 1393 (1993).

[15] R. Binder, D. Scott, A. E. Paul, M. Lindberg, K. Henneberger, and S. W. Koch, Phys. Rev. B **45**, 1107 (1992).

[16] C. T. Hultgren and E. P. Ippen, *Technical Digest of IQEC-94* (Ref. 6).

[17] K. Meissner, B. Fluegel, H. Giessen, G. Mohs, R. Binder, S W. Koch, and N. Peyghambarian, *Technical Digest of IQEC-94* (Ref. 6).

[18] M. J. LaGasse, K. K. Anderson, C. A. Wang, H. A. Haus, and J. G. Fujimto, Appl. Phys. Lett. **56**, 417 (1990).

[19] L. Banyai and S. W. Koch, Z. Phys. B **63**, 283 (1986).